


Diagnostic value of bone marrow core biopsy patterns in lymphoplasmacytic lymphoma/Waldenström macroglobulinaemia and description of its mutational profiles by targeted NGS

Julia Garcia-Reyero,¹ Nerea Martinez Magunacelaya,¹ Sonia Gonzalez de Villambrosia,¹ Angela Gomez Mediavilla,¹ Marcela Urquieta Lam,¹ Andres Insunza,¹ Raul Tonda,² Sergi Beltran,² Marta Gut,² Ainara Gonzalez,¹ Santiago Montes-Moreno ¹

► Additional material is published online only. To view, please visit the journal online (<http://dx.doi.org/10.1136/jclinpath-2019-206282>).

¹Anatomic Pathology Service, Hematology Service and Translational Hematopathology Lab, Hospital Universitario Marques de Valdecilla/IDIVAL, Centro de Investigación Biomédica en Red de Cáncer (CIBERONC), Santander, Cantabria, Spain

²Centre Nacional d'Anàlisi Genòmica (CNAG-CRG), Barcelona Institute of Science and Technology (BIST), Barcelona, Catalunya, Spain

Correspondence to

Dr Santiago Montes-Moreno, Anatomic Pathology Service and Translational Hematopathology Lab, Hospital Universitario Marques de Valdecilla/IDIVAL, Santander 39008, Spain; santiago.montes@scsalud.es

JG-R and NMM contributed equally.

Received 20 October 2019

Revised 7 January 2020

Accepted 9 January 2020

Published Online First

24 January 2020



© Author(s) (or their employer(s)) 2020. No commercial re-use. See rights and permissions. Published by BMJ.

To cite: Garcia-Reyero J, Martinez Magunacelaya N, Gonzalez de Villambrosia S, et al. *J Clin Pathol* 2020;**73**:571–577.

ABSTRACT

Aims The aim of this study was to describe the characteristics of the bone marrow infiltration found in a series of clinically defined lymphoplasmacytic lymphoma (LPL)/Waldenström macroglobulinaemia (WM) and IgM-monoclonal gammopathy of undetermined significance (MGUS) and to perform a targeted next-generation sequencing (NGS) for the identification of additional somatic mutations to *MYD88p.L265P* in LPL/WM.

Methods We have reviewed a series of 35 bone marrow biopsies from 28 patients with a clinical diagnosis of LPL/WM (24 cases) or MGUS (4 cases). Bone marrow infiltration characteristics by morphology, immunohistochemistry, flow cytometry (FCM), allele-specific real-time PCR for the detection of *MYD88p.L265P* mutation, targeted exonic amplicon-based NGS of 35 lymphoma-related genes and direct sequencing were analysed.

Results Our findings show that bone marrow trephine biopsy evaluation is superior to FCM in the identification of significant lymphoid infiltrates. A combined paratrabecular and interstitial infiltration pattern is the most common feature in LPL/WM while a patchy interstitial pattern characterises IgM-MGUS cases. *MYD88p.L265P* mutation was found by allele-specific-PCR in 92% of the LPL cases (22 out of 24) and 25% of IgM-MGUS cases (1 out of 4 cases). In addition to *MYD88p.L265P* somatic mutations in *CXCR4*, *KMT2D*, *PRDM1/Blimp1*, *MYC* and *ID3* were found by NGS and direct sequencing in 4 cases.

Conclusions In conclusion, bone marrow core biopsy evaluation is critical in the identification of unequivocal bone marrow infiltration by LPL/WM. In addition to *MYD88p.L265P*, somatic mutations in *CXCR4*, *KMT2D*, *PRDM1/Blimp1*, *MYC* and *ID3* can appear in a fraction of LPL/WM.

BACKGROUND

Lymphoplasmacytic lymphoma (LPL) is a neoplasm of small B cell lymphocytes, plasmacytoid lymphocytes and plasma cells, usually involving the bone marrow and sometimes lymph node and spleen.¹ Waldenström macroglobulinaemia (WM) is defined by the combination of an LPL with an IgM monoclonal component,² irrespective of the amount of

the monoclonal paraprotein.¹ *MYD88p.L265P* somatic mutation has been found to be the driver mutation in most cases.^{3–6}

The pattern of bone marrow infiltration in cases of LPL/WM has been previously characterised in retrospective case series with some detail,^{7,8} emphasising the differential diagnostic features with other small B cell lymphomas such as marginal zone lymphoma.⁷ On the other hand, IgM monoclonal gammopathy of undetermined significance (MGUS) has been recently incorporated in the revised version of the WHO classification of tumours.¹ This category has been also suggested to be applied in cases that may show equivocal evidence of marrow disease. In this regard, the equivalency of bone marrow aspirate cell count, the demonstration of clonal B cells by flow cytometry (FCM) or molecular methods and bone marrow trephine infiltration patterns and cellular quantification is controversial.

The aim of this study was to describe the characteristics of the bone marrow infiltration in clinically defined LPL/WM and IgM-MGUS performing a correlation study between the bone marrow trephine biopsy patterns of infiltration and the results from immunohistochemistry (IHC), FCM and molecular testing for the detection of *MYD88p.L265P* mutation. In addition, we have performed targeted next-generation sequencing (NGS) and direct sequencing for the identification of additional somatic mutations in candidate genes relevant for lymphoma pathogenesis in a subset of cases.

METHODS

Case selection

Thirty-one samples from 24 patients with LPL/WM and 4 cases diagnosed as IgM-MGUS were obtained retrospectively from the files of the Anatomic Pathology Department of the Hospital Universitario Marqués de Valdecilla. In addition, a series of 47 bone marrow trephine biopsies from patients with a diagnosis of marginal zone lymphoma (MZL, 24 cases) and chronic lymphocytic leukaemia (CLL, 23 cases) were reviewed. Clinical data were retrieved in all cases (see summary in [table 1](#)). Details about case and tissue procurement can be found in online supplementary material.

Table 1 Summary of clinical characteristics of the patients

Gender (male/female)	20/8
Age (median, range)	72 (49–89)
Diagnosis	
IgM-MGUS	4 cases
Smouldering LPL/WM	5 cases
LPL/WM	19 cases
LPL/WM cases—clinical signs and symptoms	
Anaemia	13/19 cases (65%)
Asthenia, weight loss, fever	12/19 cases (60%)
Headache	6/19 cases (30%)
Vision changes	2/19 cases (10%)
Hyperviscosity-related symptoms	10/19 (50%)
Amyloid deposits	0/19 (0%)
Neuropathy	5/19 (25%)
Palpable splenomegaly	2/19 (10%)
Hepatomegaly	4/19 (20%)
Lymph node involvement	9/19 (45%)
Extranodal involvement	3/19 (15%)
Cryoglobulinaemia	1/19 (5%)
Hepatitis C virus	0/19 (0%)

LPL, lymphoplasmacytic lymphoma; MGUS, monoclonal gammopathy of undetermined significance; WM, Waldenström macroglobulinaemia.

Morphology, immunohistochemistry and fluorescent in situ hybridisation: conventional karyotyping and flow cytometry

Histopathological patterns in the bone marrow biopsy were categorised as paratrabeular, interstitial (diffuse), interstitial (nodular), interstitial (diffuse-solid), interstitial (patchy) or a combination of those. A focal infiltrate was considered paratrabeular when the contact surface of the infiltrate with the trabecular bone was larger than the maximum diameter perpendicular to the bone. Interstitial infiltrates were categorised as nodular when clearly defined focal infiltrates were found in an intertrabeular location. Diffuse infiltrates were considered patchy, diffuse or diffuse-solid according to the density of lymphoid cells

in the bone marrow stroma (see online supplementary figures 4 and 6 for details).

Immunohistochemical reactions were performed following conventional automated procedures. Conventional karyotyping and multicolour FCM were also performed using bone marrow whole cell population aspirate material (see online supplementary materials for details).

Allele-specific PCR for the detection of *MYD88*p.L265P mutation

A customised assay based on allele-specific PCR using Taqman probes (ThermoFisher) against wild-type and mutant L265P *MYD88* gene was used. Validation results against Sanger sequencing showed a specificity of 100% for the identification of *MYD88*p.L265P mutation. Detection sensitivity using formalin-fixed paraffin-embedded (FFPE) material was 5% and 1% using DNA from bone marrow aspirate fresh material.

Next-generation sequencing using amplicon-based library generation and Sanger sequencing for the detection of *CXCR4* mutation

DNA was extracted from FFPE samples or fresh bone marrow aspirate samples using the PicoPure DNA Isolation Kit (ThermoFisher Scientific) and DNA was quantified by Qbit fluorometer (ThermoFisher Scientific). All samples subjected to NGS analysis were required to have >10% of clonal B cells as identified by either FCM or IHC. Details about amplicon-based library generation, NGS and direct Sanger sequencing data interpretation and reporting can be found in online supplementary material. Finally, 16 somatic mutations (15 missense, 1 frameshift deletion) in 5 genes were considered (table 2). The complete list of genes analysed, and variants identified in the cases analysed is shown in online supplementary material and table 2.

Statistical analysis

XLSTAT Biomed software (V.19.4) was used for statistical analysis. Wilcoxon test and Pearson's correlation test were calculated. Descriptive statistics were performed.

Table 2 Summary of somatic mutations identified by targeted NGS

Case ID	Gene	Chromosome	Location	Allele	cDNA_position	AA change	VAF (NGS)	Consequence	Existing_variation
5a	<i>MYD88</i>	3	Exon 4	C	c.794T>C	265 L/P	31%	Missense/deleterious	COSM85940
5b	<i>MYD88</i>	3	Exon 4	C	c.794T>C	265 L/P	28%	Missense/deleterious	COSM85940
6	<i>MYD88</i>	3	Exon 4	C	c.794T>C	265 L/P	3%	Missense/deleterious	COSM85940
6	<i>CXCR4</i>	2	Exon 1	G	c.1025C>G	342 S342*	–†	Nonsense	COSM5981986
11	<i>MYD88</i>	3	Exon 4	C	c.794T>C	265 L/P	51%	Missense/deleterious	COSM85940
12	<i>MYD88</i>	3	Exon 4	C	c.794T>C	265 L/P	28%	Missense/deleterious	COSM85940
13a	<i>MYD88</i>	3	Exon 4	C	c.794T>C	265 L/P	59%	Missense/deleterious	COSM85940
13b	<i>MYD88</i>	3	Exon 4	C	c.794T>C	265 L/P	20%	Missense/deleterious	COSM85940
14	<i>MYD88</i>	3	Exon 4	C	c.794T>C	265 L/P	13%	Missense/deleterious	COSM85940
15	<i>MYD88</i>	3	Exon 4	C	c.794T>C	265 L/P	10%	Missense/deleterious	COSM85940
15	<i>PRDM1</i>	6	Exon 7	T	c.2251C>T	673 H/Y	28%	Missense/deleterious	–
15	<i>MYC</i>	8	Exon 3	G	c.1721A>G	404 K/R	15%	Missense/deleterious	–
19	<i>MYD88</i>	3	Exon 4	C	c.794T>C	265 L/P	24%	Missense/deleterious	COSM85940
24b	<i>MYD88</i>	3	Exon 4	C	c.794T>C	265 L/P	12%	Missense/deleterious	COSM85940
24b	<i>KMT2D</i>	12	Exon 31	T	c.7670C>T	2557 P/L	28%	Missense/deleterious	COSM1362024
24b	<i>KMT2D</i>	12	Exon 14			1379 Met1379fs	24%	Frameshift deletion/deleterious	–
21	<i>ID3</i>	1	Exon 1	T	c.376C>T	3 A/V	15%	Missense/deleterious	–

*.

†*CXCR4* mutation was detected by direct Sanger sequencing.

AA, Aminoacid; NGS, next-generation sequencing; VAF, Variant Allele Frequency.

Table 3 Summary of immunological, histopathological, phenotypic and molecular features

M protein (median, range)	2.53 g (0.17–6.47)
M protein light chain restriction	K 19 cases (68%) λ 9 cases (32%)
Bone marrow infiltration pattern, LPL cases:	
Paratrabeular and interstitial	21 samples (67%)
Paratrabeular and interstitial (patchy)	9 samples
Paratrabeular and interstitial (diffuse)	4 samples
Paratrabeular and interstitial (diffuse, nodular)	1 samples
Paratrabeular and interstitial (nodular)	7 samples
Interstitial only	10 samples (32%)
Interstitial (patchy)	3 samples
Interstitial (diffuse)	1 sample
Interstitial (nodular)	2 samples
Interstitial (diffuse-solid)	4 samples
Bone marrow infiltration pattern, IgM-MGUS cases:	
Interstitial (patchy)	4 samples (100%)
Phenotype	
CD20-positive B cells (IHC), median, range	20% (0%–80%)*
CD20-positive clonal B cells (FCM), median, range	6.6% (0%–62%)*
MYD88p.L265P mutation (AS-PCR)	
LPL	22/24 positive (92%) Median VAF 0.09% (0–0.72)
IgM-MGUS	¼ positive (25%), VAF 0.045

*Quantification of B cells by IHC using CD20 antibody showed higher median values than by FCM (p value of the median difference, Wilcoxon test <0.0001). Correlation between the quantification of B cells using CD20 IHC and the quantification of clonal B cells by FCM was significant (Pearson's correlation test 0.778, p<0.0001).

AS-PCR, allele-specific PCR; FCM, flow cytometry; IHC, immunohistochemistry; LPL, lymphoplasmacytic lymphoma.

RESULTS

A summary of the clinical features of the series can be found in [table 1](#) and online supplementary table. The cohort was composed of 28 patients, 20 male (70%) and 8 female. Median age was 72 years (range 49–89 years). Nineteen out of 28 (68%) patients fulfilled criteria for LPL/WM, 5 patients (19%) were considered asymptomatic or smouldering LPL/WM² and 4 cases were classified as IgM-MGUS. Among LPL/WM, the most common clinical presentation included anaemia (65%), constitutional symptoms (60%) and hyperviscosity-related symptoms (50%). Five patients had IgM-related neuropathy and one single patient had cryoglobulinaemia. Palpable splenomegaly was found in two patients (10%) and nodal involvement by CT scan in nine patients (45%). In three patients, lymph node biopsy confirmed involvement by LPL. None of our patients had hepatitis C virus infection.

LPL/WM shows a predominantly paratrabeular pattern combined with interstitial infiltrates; IgM-MGUS shows a patchy interstitial pattern of infiltration

LPL/WM bone marrow biopsy results are summarised in [table 3](#). LPL core biopsy samples were characterised by a paratrabeular infiltration pattern (21 samples, 67%), combined with either patchy (9 samples, 25%), nodular (7 samples, 19%) or diffuse (5 samples, 13%) interstitial patterns. The other 10 samples (32%) showed a non-paratrabeular pattern with interstitial involvement (patchy in 3 samples, nodular in 2 samples, diffuse in 1 sample, diffuse-solid in 4 samples). The samples with patchy

interstitial infiltrate derived from two patients (n10, n24) with previous pretreatment core biopsies with a significant infiltrate ([figure 1](#)). In contrast, only 6 out of 23 (25%) cases of MZL (19 cases of Splenic Marginal Zone Lymphoma (SMZL), 3 Nodal Marginal Zone Lymphoma (NMZL) and 1 case of Mucosa-Associated Lymphoid Tissue (MALT) lymphoma) showed a paratrabeular component and only 1 out of 24 (4%) cases of CLL showed this pattern. The most common infiltration pattern in MZL was interstitial and intrasinusoidal (10 samples, 42%), followed by interstitial only (8 samples, 33%). CLL cases were almost purely interstitial (22 samples, 96%) (see online supplementary table 1).

Regarding the cytological features, all cases showed the presence of small B cell lymphocytes, plasmacytoid cells and plasma cells with variable degrees of plasma cell differentiation. Dutcher bodies were present, although infrequent (online supplementary figure 3). One sample showed a complete absence of B lymphoid cells and was composed purely of plasmacytoid and plasma cells (case n4, IgM-MGUS). Mast cells were present in almost every case.

Bone marrow quantification of B cells and correlation with MYD88p.L265P allele burden determination by allele-specific-PCR

Bone marrow cells in the trephine biopsy were stained with antibodies against CD20 and CD138 and positive cells were quantified by visual estimation against the overall marrow cellularity. An estimation of the percentage of positive cells with both markers was annotated for every sample in 5% increments. The median percentage of CD20-positive cells in all 35 available samples was 20% (range 0%–80%) and the median presence of CD20-positive and CD138-positive cells was 40% (range 5%–90%). FCM performed using bone marrow aspirate material disclosed a median percentage of clonal B cells of 6.6% (range 0%–62%). Thus, quantification of B cells by IHC using CD20 antibody showed higher values than by FCM in 32 out of 35 cases (p value of the median difference, Wilcoxon test p<0.0001, see online supplementary table 1 and online supplementary figure 6). There was a high correlation between the quantification of B cells using CD20 IHC and the quantification of clonal B cells by FCM (Pearson's correlation test 0.78, p<0.0001, online supplementary figure 1).

Regarding the correlation between the amount of bone marrow infiltration by lymphoplasmacytic cells and the presence of symptoms attributable to the disease, we found no difference between smouldering LPL cases and LPL/WM cases. As shown in the online supplementary table, smouldering LPL cases (6, 7, 14, 23, 28) had a median % of B cells by IHC of 20 (range 10–35) and by FCM of 6.6 (range 1.6–18.5). The same median values were obtained for the 19 LPL/WM cases.

In addition, we performed tryptase staining in 18 samples. In five samples (28%), mast cells comprised <5% of the bone marrow cellularity. In 13 samples (72%), it was between 5% and 10% of the cellularity. DBA44 was also performed in 15 cases. In five cases, DBA44 staining was in the range of 1%–5% of the cellularity; in 10 cases it was negative.

After allele-specific PCR (AS-PCR), 22 out of 24 LPL/WM cases (92%) were positive for MYD88p.L265P mutation. In one out of two of the negative cases, the quantification of clonal B cells in the sample analysed was below the detection limit of the technique, thus a false-negative result could not be ruled out. Median variant allele frequency (ie, the fraction of mutated

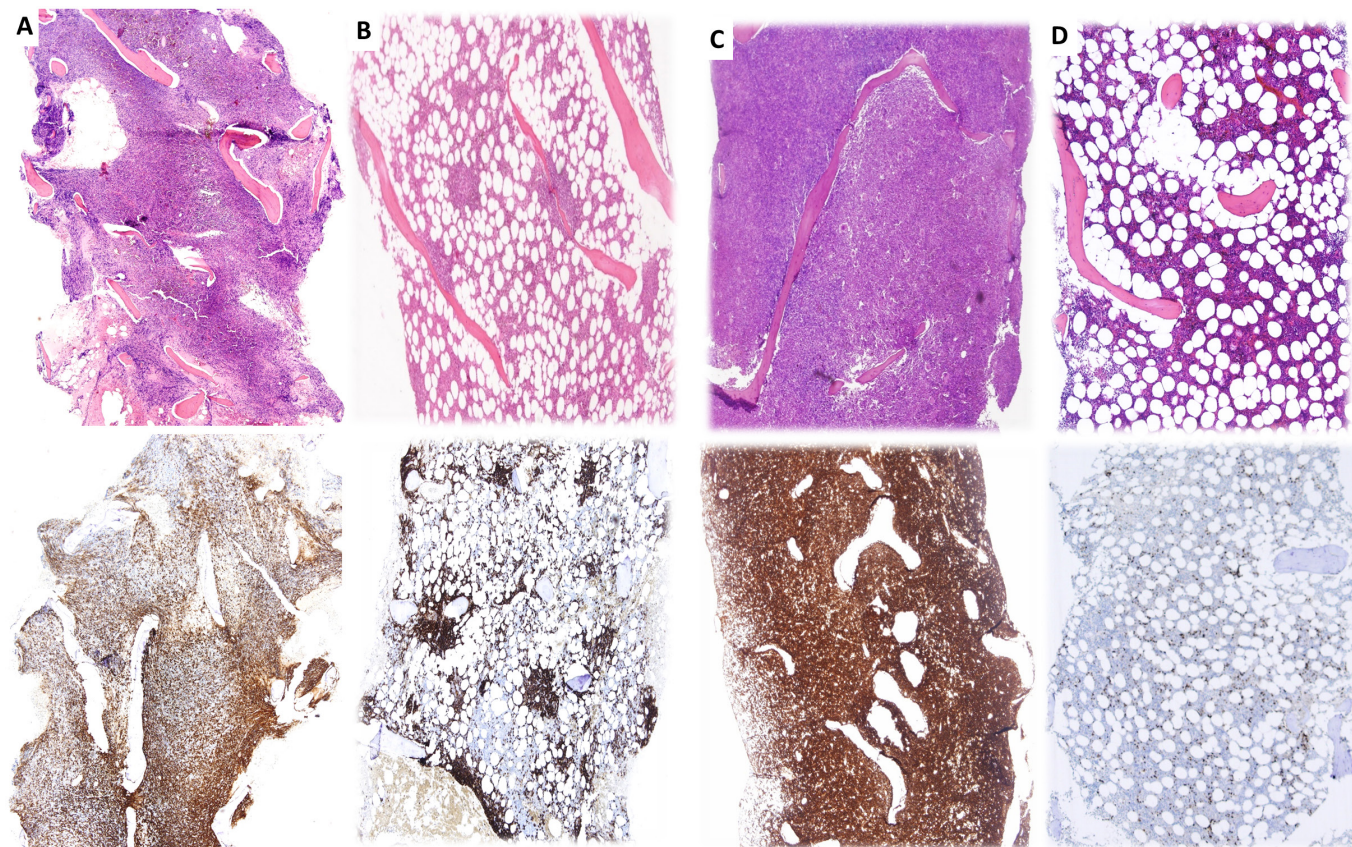


Figure 1 Main histopathological patterns. Bone marrow core biopsy infiltration patterns as shown with H&E and CD20 IHC. (A) Paratrabecular and interstitial-diffuse; (B) paratrabecular and interstitial-nodular; (C) diffuse interstitial-solid; (D) patchy interstitial.

DNA in the total DNA present in a given sample) of the mutated LPL cases was 9% (range 0%–72%). One out of four (25%) IgM-MGUS cases was positive with a VAF of 4%. Correlation between the AS-PCR values from 27 samples with positive results for both AS-PCR and FCM was significant (Spearman's correlation value 0.477, $p=0.013$, online supplementary figure 2A), as it was the comparison between AS-PCR and IHC (Spearman's correlation value 0.457, $p=0.017$, online supplementary figure 2B).

Genetic characterisation of LPL: additional genetic events to *MYD88p.L265P* mutation include *CXCR4*, *KMT2D*, *PRDM1* and *MYC* mutations

Targeted NGS was performed with a customised amplicon-based NGS protocol using DNA from FFPE or aspirate bone marrow samples. Thirteen samples from 11 patients with a significant neoplastic infiltration ($\geq 10\%$ by FCM/IHC) were included in this analysis. A summary of the results is shown in figure 2 and table 2. Nine out of 11 cases were *MYD88p.L265P* mutated and 2 cases were negative (n21, n22). In six out of these nine cases, only *MYD88p.L265P* mutation was found after targeted NGS. The other two cases had additional mutations in *PRDM1*, *MYC* (case n15) and *KMT2D* (case n24). One of the two *MYD88* wild-type cases had mutations in *ID3*. After direct Sanger sequencing, one (case n6) out of four analysed cases (25%) was found to harbour the *CXCR4* c.1025 C>G (p.S342*) mutation (online supplementary material). The lack of detection of this particular mutation in this case by targeted NGS was probably due to a drop-off NGS artefact.

Recurrent mutations, different than *MYD88p.L265P* were found in *KMT2D*. Interestingly, one case (n24) had two different *KMT2D* mutations (one frameshift deletion in exon 14 and one missense single nucleotide mutation (c.7670C>T) in exon 31). A possible mechanism of *KMT2D* biallelic inactivation is suggested based on this pattern of *KMT2D* mutations.

In addition, 6q deletion was studied in nine cases by conventional interphase fluorescent in situ hybridisation (FISH) and/or conventional karyotyping. 6q deletion was found in five out of nine cases (55%, n5, n12, n13, n14 and n25). All five cases were *MYD88p.L265P* mutated.

CONCLUSIONS

The diagnosis of LPL/WM according to the updated WHO classification relies on the identification of a significant bone marrow infiltration by LPL clonal B cells. The category of IgM-MGUS has been incorporated to classify those cases that do not have unequivocal bone marrow infiltration.¹ An arbitrary cut-off of 10% clonal lymphoplasmacytic cells has been designated as the threshold to identify an LPL infiltrate as significant. However, discordant results can be found when analysing the bone marrow infiltration with different available methods including morphological assessment of the bone marrow aspirate and bone marrow biopsy, identification of clonal B cell populations by FCM and clonality studies.^{2,9} To date, no study has analysed the correlation between the different methods used in these multiparametric approach using new available molecular tools in the framework of the revised WHO classification. The aim of this study was to characterise and correlate the results of

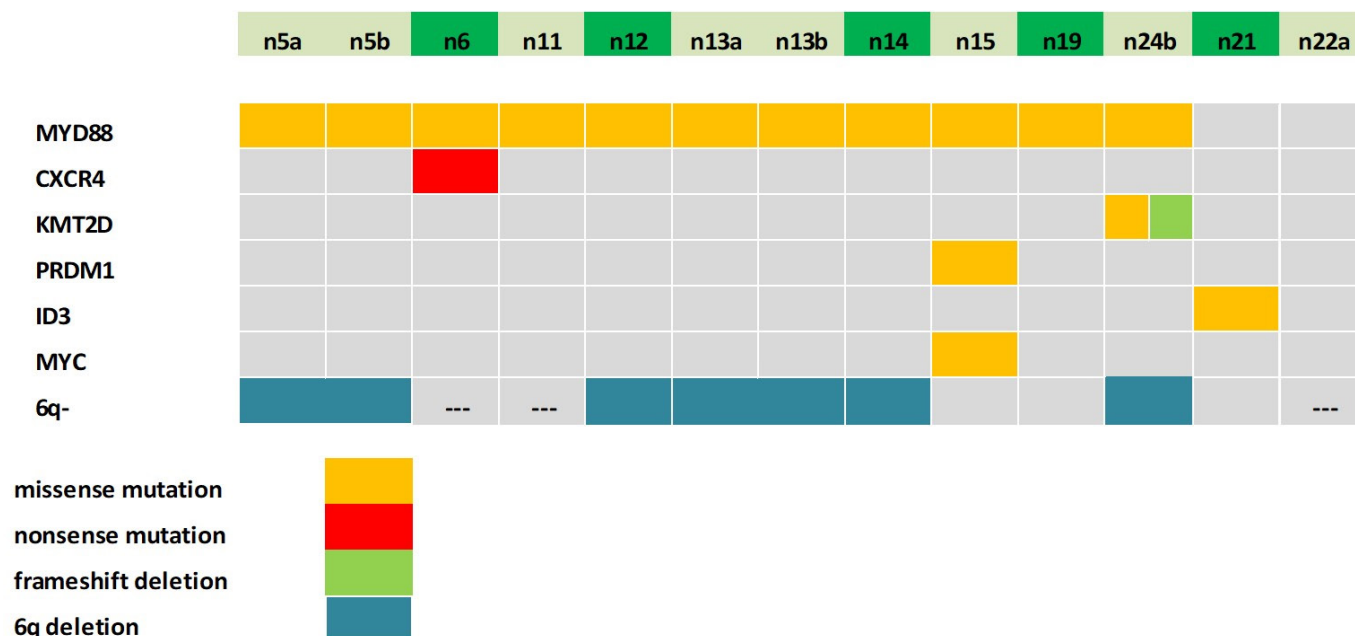


Figure 2 Mutational profiles of lymphoplasmacytic lymphoma/Waldenström macroglobulinaemia. After targeted next-generation sequencing with a lymphoma dedicated panel of genes, we found additional somatic mutations to *MYD88*p.L265P in roughly one-fourth of the cases (3 out of 11 cases). Co-mutated genes were *MYD88* and *KMT2D* and *MYD88*, *PRDM1* and *MYC*. Interestingly, one *MYD88* wild-type case had a mutation in *ID3*. 6q deletion was found in five out of nine cases (55%). All five cases were *MYD88*p.L265P mutated.

these complementary methods in a series of patients in order to optimise the identification of patients with LPL/WM who may require therapeutic intervention. In addition, we have expanded the genetic characterisation of our cases to identify coexisting genetic events in the disease.

Morphological assessment of the bone marrow infiltration pattern in the trephine core biopsy showed that a combined paratrabeular and interstitial pattern was the most common feature in LPL cases, with 60% of the cases showing different combinations of patterns. In contrast, MZL and CLL cases in our study showed predominantly interstitial patterns, combined with intrasinusoidal growth in the case of MZL. These results are in contrast with the traditional concept of a interstitial pattern of bone marrow involvement in LPL cases.¹ Recent reports have shown a similar result to ours, with a relatively high frequency of paratrabeular involvement in LPL cases, both *MYD88* mutated and wild type.^{8–10} Interestingly, this morphological feature has also been found by others as a significant differential feature with marginal zone B cell lymphoma involving the bone marrow.⁷ Thirty-two per cent of our LPL samples showed a non-paratrabeular pattern with interstitial infiltration. Only three of the samples showed a limited patchy interstitial infiltrate and these samples derived from patients after initial therapy. In contrast to LPL cases, all four cases with IgM-MGUS showed a limited patchy interstitial infiltrate. Although the number of IgM-MGUS cases here analysed is relatively small, our results suggest that a patchy interstitial infiltrate is the tissue correlate of IgM-MGUS. Adequate IHC analysis is required to identify this pattern in cases of pretreatment bone marrow samples with suspected IgM-MGUS. Interestingly, this pattern can also be found in samples with low tumour burden after therapy.

Regarding the phenotypic evaluation of LPL infiltrates, there was a good correlation between the quantification of clonal B cells by FCM and the estimation of B cells in the core biopsy sample by IHC. Importantly, bone marrow core biopsy rendered in most cases a higher value than by FCM and this difference was

significant. Interestingly, in 14 out of 24 patients FCM quantification of clonal B cells was below the 10% threshold while the quantification by IHC in the bone marrow core biopsy was sufficient to meet the criteria for LPL according to WHO classification.¹ Five out of these 14 patients were considered smouldering LPL. Thus, our results suggest that it is worthwhile to evaluate the presence of neoplastic B cell infiltrates by IHC in the core biopsy samples to improve the detection of LPL cases. A possible explanation for these differences might be the preferential distribution of the LPL infiltrates in the paratrabeular regions and its association with reticulin fibrosis. This topography may prevent the aspiration the neoplastic infiltrate and its underestimation by FCM using bone marrow aspirate material. On the other hand, the multifocality and heterogeneous distribution of the infiltrate in the trephine biopsy may explain some discrepant results in few cases after serial sections of the material for downstream molecular methods.

We identified *MYD88*p.L265P somatic mutation by AS-PCR in 22 out of 24 LPL cases (92%) and one additional case of IgM-MGUS. This prevalence of *MYD88*p.L265P mutation is like previously reported cohorts.^{5–6, 11–15} Interestingly, AS-PCR quantitative results correlated well with the clonal B cell quantification by FCM and IHC of the bone marrow aspirate samples, providing an acceptable method for the quantification of the neoplastic population by molecular methods. AS-PCR and targeted NGS were concordant for the detection of *MYD88*p.L265P mutation in 20 out of 21 tested samples (92%) in our series. No other *MYD88* mutations were found after targeted NGS of *MYD88* exonic regions in our cases. Previously reported data have shown rates up to 31% of false-negative results using targeted NGS when compared with AS-PCR.^{13, 16}

After targeted NGS with a lymphoma dedicated panel of genes, we found additional somatic mutations to *MYD88*p.L265P in roughly one-fourth of the cases (3 out of 11 cases). Direct Sanger sequencing was required to identify *CXCR4* mutation in one additional case. Co-mutated genes were *MYD88* and

CXCR4, *MYD88* and *KMT2D* and *MYD88*, *PRDM1* and *MYC*. Interestingly, one *MYD88* wild-type case had a missense mutation in *ID3*. Except for *CXCR4*, *KMT2D* and *PRDM1* mutations, *MYC* and *ID3* have not been previously described in the disease. The VAF of these novel mutations is concordant with the clonal B cell fraction found in the samples by phenotyping and consistent with a derivation from the LPL clonal B cells.

CXCR4 mutations have been associated with worse outcome for patients with LPL/WM.^{5,17} A recent phase III trial suggests that *CXCR4* mutations do not alter overall survival or progression-free survival in patients treated with a combination including ibrutinib plus rituximab but evidence is limited.¹⁸

KMT2D somatic mutations have been previously found in both *MYD88*p.L265P mutated and wild-type cases. The prevalence is roughly 20%–25% and some groups reported a higher incidence in *MYD88*p.L265P wild-type cases¹⁹ when compared with *MYD88*p.L265P mutated cases. It has been found at subclonal levels in *MYD88*p.L265P mutated cases.¹³ Its relatively high prevalence in LPL cases suggests a potential role in the pathogenesis of the disease. Interestingly, *KMT2D* germline mutations have been found to be associated with Kabuki syndrome²⁰ and *KMT2D* knockout in mice leads to reduced class-switched B cell populations following immunisation, consistent with defective terminal B cell differentiation^{21,22} and mirroring the immune deficiency found in patients with Kabuki syndrome.

Regarding *PRDM1* mutations, we have identified a somatic missense mutation located in exon 7 of the gene (c.2251C>T; H673Y) that involves the Zn finger domain, responsible of transcriptional regulation of *PRDM1*/Blimp1 protein target genes. This mutation has been identified previously by our group in a case of plasmablastic lymphoma.²³ *PRDM1* gene has been found mutated in ~8% of overall diffuse large B cell lymphoma.^{24,25} Furthermore, it has been found to be inactivated, either by mutation or genetic deletion of 6q21-q22.1 locus, in a significant fraction (23%–24%) of ABC-type Diffuse Large B cell Lymphoma (DLBCL).^{26,27} Recently, *PRDM1* has been found mutated in 4% of cases of WM.¹³ Importantly, in our series, the case with the *PRDM1*/Blimp1 mutation showed a normal pattern for 6q by FISH ruling out biallelic inactivation of *PRDM1*/Blimp1.

In summary, bone marrow core biopsy evaluation is critical in the identification of unequivocal bone marrow infiltration by LPL/WM. A combined paratrabecular and interstitial infiltration pattern is the most common feature in LPL/WM while a patchy interstitial pattern characterises IgM-MGUS cases. It is particularly relevant in the framework of the revised WHO classification to differentiate between patients with IgM-MGUS and LPL in order identify those that may require therapeutic intervention. Furthermore, the use of targeted NGS and direct

sequencing confirms the relatively uniform molecular profiles of the disease, characterised by *MYD88*p.L265P mutation and occasional somatic mutations in *CXCR4*, *KMT2D*, *PRDM1*/Blimp1, *MYC* and *ID3* in a fraction of patient samples with LPL/WM.

Handling editor Mary Frances McMullin.

Acknowledgements The authors want to acknowledge the Valdecilla Tumor Biobank Unit (Tissue Node, PT13/0010/0024) for their skilful handling of tissue samples.

Contributors JG-R, NMM, AGM, AG, RT, SB and MG performed research. SGdV, MUL and AI provided clinical data. SM-M designed research, performed research and wrote the manuscript. All authors approved the manuscript.

Funding This study was supported by grants from MINECO (PI16/1397, SMM, Principal Investigator) and IDIVAL (NEXTVAL 15/09, SMM, Principal Investigator). NMM was supported by Asociación Española contra el Cancer (AECC).

Competing interests None declared.

Patient consent for publication Not required.

Ethics approval The study and sample collection were approved by the local ethics committee (CEIC Cantabria) and complies with the Declaration of Helsinki. Informed written consent was obtained when required.

Provenance and peer review Not commissioned; externally peer reviewed.

Data availability statement All data relevant to the study are included in the article or uploaded as supplementary information.

ORCID iD

Santiago Montes-Moreno <http://orcid.org/0000-0002-3565-8262>

REFERENCES

- 1 Swerdlow SH CE, Harris NL, Jaffe ES, *et al*, eds. *WHO Classification of Tumours of Haematopoietic and Lymphoid Tissues (revised 4th edition)*. Lyon: IARC, 2017.
- 2 Owen RG, Treon SP, Al-Katib A, *et al*. Clinicopathological definition of Waldenström's macroglobulinemia: consensus panel recommendations from the second International workshop on Waldenström's macroglobulinemia. *Semin Oncol* 2003;30:110–5.
- 3 Hunter ZR, Xu L, Yang G, *et al*. Transcriptome sequencing reveals a profile that corresponds to genomic variants in Waldenström macroglobulinemia. *Blood* 2016;128:827–38.
- 4 Hunter ZR, Xu L, Yang G, *et al*. The genomic landscape of Waldenström macroglobulinemia is characterized by highly recurring MyD88 and WHIM-like CXCR4 mutations, and small somatic deletions associated with B-cell lymphomagenesis. *Blood* 2014;123:1637–46.
- 5 Treon SP, Cao Y, Xu L, *et al*. Somatic mutations in MYD88 and CXCR4 are determinants of clinical presentation and overall survival in Waldenström macroglobulinemia. *Blood* 2014;123:2791–6.
- 6 Treon SP, Xu L, Yang G, *et al*. MYD88 L265P somatic mutation in Waldenström's macroglobulinemia. *N Engl J Med* 2012;367:826–33.
- 7 Bassarova A, Trøen G, Spetälén S, *et al*. Lymphoplasmacytic lymphoma and marginal zone lymphoma in the bone marrow: paratrabecular involvement as an important distinguishing feature. *Am J Clin Pathol* 2015;143:797–806.
- 8 Fang H, Kapoor P, Gonsalves WL, *et al*. Defining lymphoplasmacytic lymphoma: does MYD88L265P define a pathologically distinct entity among patients with an IgM paraprotein and bone marrow-based low-grade B-cell lymphomas with Plasmacytic differentiation? *Am J Clin Pathol* 2018;150:168–76.
- 9 Feiner HD, Rizk CC, Finfer MD, *et al*. IgM monoclonal gammopathy/Waldenström's macroglobulinemia: a morphological and immunophenotypic study of the bone marrow. *Mod Pathol* 1990;3:348–56.
- 10 King RL, Gonsalves WL, Ansell SM, *et al*. Lymphoplasmacytic lymphoma with a Non-IgM paraprotein shows clinical and pathologic heterogeneity and may harbor MYD88 L265P mutations. *Am J Clin Pathol* 2016;145:843–51.
- 11 Castillo JJ, Garcia-Sanz R, Hatjiharissi E, *et al*. Recommendations for the diagnosis and initial evaluation of patients with Waldenström macroglobulinaemia: a task force from the 8th International workshop on Waldenström macroglobulinaemia. *Br J Haematol* 2016;175:77–86.
- 12 Xu L, Hunter ZR, Yang G, *et al*. MYD88 L265P in Waldenström macroglobulinemia, immunoglobulin M monoclonal gammopathy, and other B-cell lymphoproliferative disorders using conventional and quantitative allele-specific polymerase chain reaction. *Blood* 2013;121:2051–8.
- 13 Varettoni M, Zibellini S, Defrancesco I, *et al*. Pattern of somatic mutations in patients with Waldenström macroglobulinemia or IgM monoclonal gammopathy of undetermined significance. *Haematologica* 2017;102:2077–85.
- 14 Ondrejka SL, Lin JJ, Warden DW, *et al*. MYD88 L265P somatic mutation: its usefulness in the differential diagnosis of bone marrow involvement by B-cell lymphoproliferative disorders. *Am J Clin Pathol* 2013;140:387–94.

Take home messages

- Bone marrow core biopsy evaluation is critical in the identification of unequivocal bone marrow infiltration by lymphoplasmacytic lymphoma (LPL)/Waldenström macroglobulinaemia (WM).
- A combined paratrabecular and interstitial infiltration pattern is the most common feature in LPL/WM while a patchy interstitial pattern characterises IgM-monoclonal gammopathy of undetermined significance cases.
- Somatic mutations in *CXCR4*, *KMT2D*, *PRDM1*/Blimp1, *MYC* and *ID3* can be found in a fraction of LPL/WM in addition to *MYD88*p.L265P.

- 15 Jiménez C, Sebastián E, Chillón MC, *et al.* MYD88 L265P is a marker highly characteristic of, but not restricted to, Waldenström's macroglobulinemia. *Leukemia* 2013;27:1722–8.
- 16 Amanda Kofides M, Xia Liu MS, Christopher Patterson MD. Alternative Mutations and Isoform Dysregulation in MYD88 in Waldenström's Macroglobulinemia. ASH Annual Meeting, San Diego, USA, 2018.
- 17 Sklavenitis-Pistofidis R, Capelletti M, Liu C-J, *et al.* Bortezomib overcomes the negative impact of CXCR4 mutations on survival of Waldenström macroglobulinemia patients. *Blood* 2018;132:2608–12.
- 18 Dimopoulos MA, Tedeschi A, Trotman J, *et al.* Phase 3 trial of ibrutinib plus rituximab in Waldenström's macroglobulinemia. *N Engl J Med* 2018;378:2399–410.
- 19 Hunter ZR, Xu L, Tsakmaklis N, *et al.* Insights into the genomic landscape of MYD88 wild-type Waldenström macroglobulinemia. *Blood Adv* 2018;2:2937–46.
- 20 Lindsley AW, Saal HM, Burrow TA, *et al.* Defects of B-cell terminal differentiation in patients with type-1 Kabuki syndrome. *J Allergy Clin Immunol* 2016;137:179–87.
- 21 Zhang J, Dominguez-Sola D, Hussein S, *et al.* Disruption of KMT2D perturbs germinal center B cell development and promotes lymphomagenesis. *Nat Med* 2015;21:1190–8.
- 22 Ortega-Molina A, Boss IW, Canela A, *et al.* The histone lysine methyltransferase KMT2D sustains a gene expression program that represses B cell lymphoma development. *Nat Med* 2015;21:1199–208.
- 23 Montes-Moreno S, Martinez-Magunacelaya N, Zecchini-Barrese T, *et al.* Plasmablastic lymphoma phenotype is determined by genetic alterations in MYC and PRDM1. *Mod Pathol* 2017;30:85–94.
- 24 Pasqualucci L, Trifonov V, Fabbri G, *et al.* Analysis of the coding genome of diffuse large B-cell lymphoma. *Nat Genet* 2011;43:830–7.
- 25 Zhang J, Grubor V, Love CL, *et al.* Genetic heterogeneity of diffuse large B-cell lymphoma. *Proc Natl Acad Sci U S A* 2013;110:1398–403.
- 26 Pasqualucci L, Compagno M, Houldsworth J, *et al.* Inactivation of the PRDM1/BLIMP1 gene in diffuse large B cell lymphoma. *J Exp Med* 2006;203:311–7.
- 27 Tam W, Gomez M, Chadburn A, *et al.* Mutational analysis of PRDM1 indicates a tumor-suppressor role in diffuse large B-cell lymphomas. *Blood* 2006;107:4090–100.